Наносистеми, наноматеріали, нанотехнології
Nanosystems, Nanomaterials, Nanotechnologies
2011, т. 9, № 4, сс. 819–830

PACS numbers: 42.70.-a, 72.40.+w, 73.40.Lq, 73.50.Pz, 84.60.Jt, 88.40.H-, 88.40.J-

Simulation Study of *n*-ZnO/*p*-Si Heterojunction Solar Cell

A. D. Pogrebnyak, N. Y. Jamil*, and A. K. M. Muhammed

Sumy State University,
2 Rimsky-Korsakov Str.,
UA-40007 Sumy, Ukraine
**University of Mosul,*
St. Culture,
Mosul, Iraq

In a given paper, the simulation program SCAPS–10 is used to study the structure of the *n*-ZnO/*p*-Si heterojunction solar cell. This program is designed basically for the simulation and studying the properties of photonic devices. We explored such important controllable design parameters affecting the performance of the *p*–*n*-junction solar cells as operating temperature, as we notice increasing in *J*–*V* characteristics with *T* increasing, the effect of thickness of each layer on the performance of a cell is studied, as well as an increasing of *J*–*V* characteristics with increasing of *p*-layer thickness. In the numerical example, 3 um *p*-layer and 3 um *n*-layer work to the best advantage for a given doping density. If we change the optimum value, the efficiency can reach $\eta = 5.83\%$ with $V_{oc} = 0.589$ V, $J_{sc} = 12.451$ mA at 300 K, $Na = Nd = 10^{19}$; in this case, we have come out the optimum parameters to achieve the best performance of this type of a cell, and we made comparison with a practical ZnO/Si cell.

У даній роботі програма моделювання SCAPS-10 використовується для вивчення структури *n*-ZnO/*p*-Si-гетеропереходу сонячних елементів. Ця програма призначена в основному для моделювання та вивчення властивостей фотонних пристроїв. Ми досліджували важливі контрольовані параметри дизайну, що впливають на діяльність *p*–*n*-переходу сонячних елементів, такі як робоча температура, тому що ми побачили підвищення характеристики *J*–*V* за рахунок збільшення *T*, а також вивчили вплив товщини кожного шару на ефективність сонячного елементу і помітили підвищення *J*–*V*-характеристики зі збільшенням товщини *p*-шару. У прикладі з оптимальними параметрами товщини шару $p = 3$ мм, $n = 3$ мм, $Na = Nd = 10^{19}$ при 300 К одержали такі результати: $\eta = 5.83\%$, $V_{oc} = 0{,}589$ В, $J_{SC} = 12{,}451$ мкА/см^2; в даному випадку ми підібрали оптимальні параметри для досягнення максимальної продуктивности цього типу гетеропереходів і зробили порівняння з практичною *n*-ZnO/*p*-Si-коміркою соня-

чного елементу.

В данной работе программа моделирования SCAPS-10 используется для изучения структуры n-ZnO/p-Si-гетероперехода солнечных элементов. Эта программа предназначена в основном для моделирования и изучения свойств фотонных устройств. Мы исследовали важные контролируемые параметры дизайна, влияющие на работу p–n-перехода солнечных элементов, такие как рабочая температура, поскольку мы обнаружили повышение характеристики J–V за счёт увеличения T, изучили влияние толщины каждого слоя на эффективность солнечного элемента и увидели повышение J–V-характеристики с увеличением толщины p-слоя. В примере с оптимальными параметрами толщины слоя $p = 3$ мм, $n = 3$ мм, $\mathrm{Na} = \mathrm{Nd} = 10^{19}$ при 300 К мы получили такие результаты: $\eta = 5{,}83\%$, $V_{\mathrm{oc}} = 0{,}589$ V, $J_{\mathrm{SC}} = 12{,}451$ мкА/см^2; в данном случае мы подобрали оптимальные параметры для достижения максимальной производительности этого типа гетеропереходов и сделали сравнение с практической n-ZnO/p-Si-ячейкой солнечного элемента.

Key words: simulation program SCAPS-10, n-ZnO/p-Si heterojunction, solar cell, operating temperature, thickness, doping density.

(Received August 23, 2011; in revised version December 15, 2011)

1. INTRODUCTION

The solar cell n-ZnO/p-Si heterojunction are used in this paper. They are basically constructed from zinc oxide (n-ZnO), which used as a window, and silicon (p-Si), used as an absorber layer for the incoming light [1].

Heterojunction solar cell have the potential to achieve the goals of higher efficiency, reliability, and lower cost, necessary for the large scale applications, for solar cell application and photodetector, using other semiconductors than silicon, which have an energy gap between 1.1 and 1.6 eV [2].

Among many different low-cost solar cell structures, one interesting heterojunction solar cell is the transparent conducting oxide (TCO) semiconductor heterojunction. The conducting oxides, including oxide semiconductors such as indium oxide (In_2O_3), tin oxide (SnO_2), and zinc oxide (ZnO), thin film ZnO, have attracted much attention because of its lower material cost and good electrical/optical properties compared to other oxides [3, 4]. Zinc oxide (ZnO) film with a large band gap of about 3.3 eV is one of the most potential materials for being used as a TCO because of its good electrical and optical properties, abundance in nature, absence of toxicity [5], and the ability to deposit these films at relatively low temperatures [4].

The oxygen vacancies and/or zinc interstitials correspond to the n-

type conductivity of the ZnO films.

2. DEVICE SIMULATION

Simulation program SCAPS-10 is used to study the structure of *n*-ZnO/*p*-Si as a solar cell. SCAPS-10 is Windows application program developed at the University of Gent with Lab Windows/CVI of National Instruments under Marc Burgelman. The program organized in a number of panels in which the user can set parameters or in which results are presented [5]. It has been developed to simulate realistically the electrical characteristics (dc and ac) of thin film heterojunction solar cells. It has been tested extensively for thin film CdTe and Cu(In,Ga)Se_2 solar cells [6].

3. RESULTS AND DISCUSSION

In energy band diagram of the *n*-ZnO/*p*-Si structure under equilibrium condition, the Fermi level will be constant through the band diagram as shown in Fig. 1.

4. EFFECT OF OPERATING TEMPERATURE

In a solar cell, the operating temperature plays a vital role in the performance. The impact of increasing temperature on light J–V curve of the *n*-ZnO/*p*-Si solar cell is shown in Fig. 2; the temperature varied as 280–380 K.

V_{oc} decreases with the increased temperature because of the temperature dependence of the reverse saturation current. The band gap energy has been slightly narrowed, and this may accelerate the recombi-

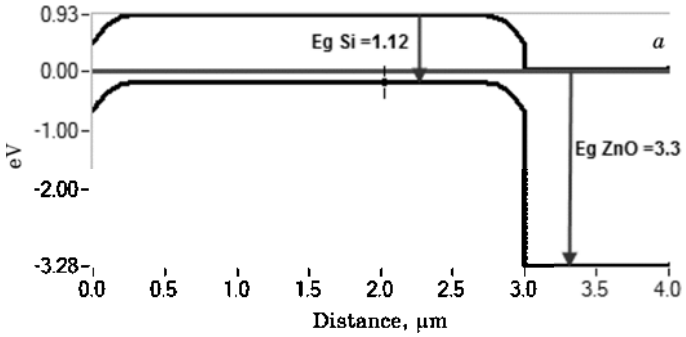

Fig. 1. Energy band diagram of *n*-ZnO/*p*-Si heterojunction solar cell under equilibrium condition.

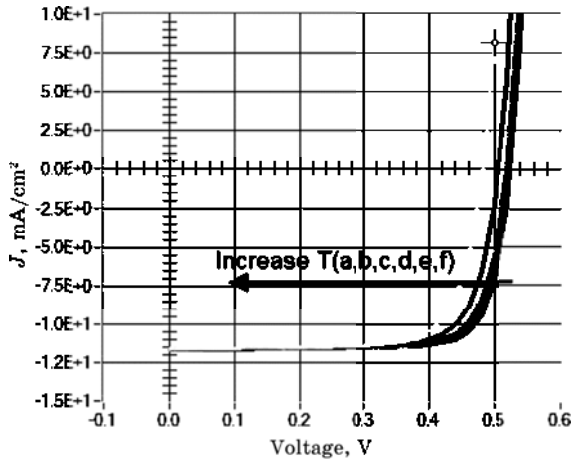

Fig. 2. J–V parameters of n-ZnO/p-Si solar cell at various temperatures: a = 280 K, b = 300 K, c = 320 K, d = 340 K, e = 360 K, f = 380 K.

nation of the EHP between the conduction band and the valance band. Although more free electrons are produced into the conduction band, the band gap energy at high temperature is unstable that may lead to recombination of electrons and holes, while travelling across the regions. So, J_{sc} is slightly decreased. The dependence of (FF%) on the operating temperature can be derived from the V_{oc} dependent on the temperature. The reduction in J_{sc} and V_{oc} with temperature leads to reduction in the efficiency with the temperature. The dependence of the output parameters on the operating temperature is listed in Table 1.

TABLE 1. J–V parameters of n-ZnO/p-Si solar cell at various temperatures.

No.	T, K	V_{oc}, Volt	J_{sc}, mA/cm^2	FF, %	η, %
a	280	0.5252	11.69	78.95	4.85
b	300	0.525	11.67	78.52	4.81
c	320	0.524	11.66	78.01	4.77
d	340	0.52	11.64	77.11	4.67
e	360	0.5	11.62	76.21	4.49
f	380	0.48	11.6	74.77	4.18

5. EFFECT OF THICKNESS

5.1. Effect of p-Si Thickness

The effect of the Si absorber layer thickness on the light J–V curves is

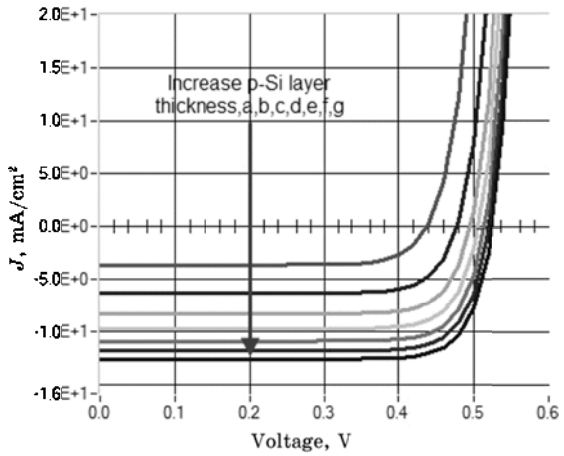

Fig. 3. *J*–*V* parameters of *n*-ZnO/*p*-Si solar cell at various Si absorber layer thickness: $a = 0.1$ um, $b = 0.5$ um, $c = 1$ um, $d = 1.5$ um, $e = 2$ um, $f = 2.5$ um, $g = 3$ um; *n*-layer = 3 um; Na = Nd = 10^{19}.

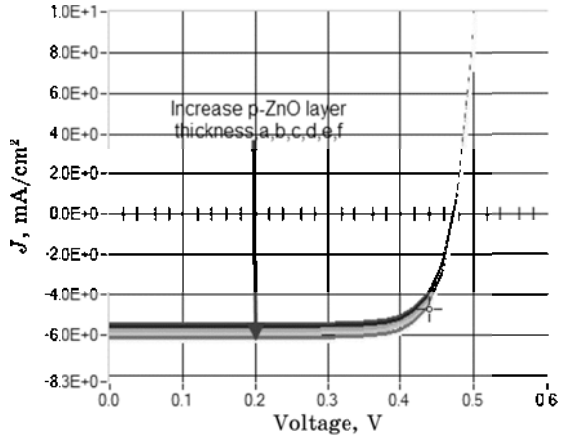

Fig. 4. *J*–*V* parameters of *n*-ZnO/*p*-Si solar cell at various ZnO absorber layer thickness: $a = 0.1$ um, $b = 0.3$ um, $c = 0.5$ um, $d = 075$ um, $e = 1$ um, $f = 2$ um.

shown in Figs. 3, 4.

The thickness of Si layer has been varied from 0.1 um to 3 um. It is clearly shown that both V_{oc} and J_{sc} have been increased as the thickness of the *p*-Si absorber layer increased. When the thickness of *p*-Si increases, this will allow the longer wavelength of the illumination to be absorbed, which, in turn, contributes in EHP generation. If the absorber layer thickness reduced, the high-recombination back-contact region will be very close to the depletion region. Thus, electrons will be captured easily by the back contact for the recombination process;

therefore, fewer electrons will contribute in EHP generation. The increment in V_{oc} and J_{sc} will increase both FF% and η%. The effect of the thickness of the *p*-Si absorber layer on the output parameters is listed in Table 2.

TABLE 2. *J*–*V* parameters of *n*-ZnO/*p*-Si solar cell at various Si absorber layer thickness.

No.	Thickness of Si, um	V_{oc}, Volt	J_{sc}, mA/cm^2	FF, %	η, %
a	0.1	0.438	3.639	76.44	1.2
b	0.5	0.477	6.32	78.43	2.3
c	1	0.495	8.336	79.26	3.2
d	1.5	0.506	9.765	79.74	3.9
e	2	0.514	10.882	79.96	4.4
f	2.5	0.52	11.799	80.21	4.9
g	3	0.525	12.578	80.35	5.3

The effect of the thickness of *p*-Si absorber layer on quantum efficiency is shown in Figs. 5, 6.

As we said, the longer-wavelengths photon will be absorbed deeper within the *p*-Si layer, so the effect of the thickness of *p*-Si layer on the quantum efficiency has been occurred in the region extended to λ = 380–1200 nm.

When the thickness of *p*-Si absorber layer increases, this will allow a

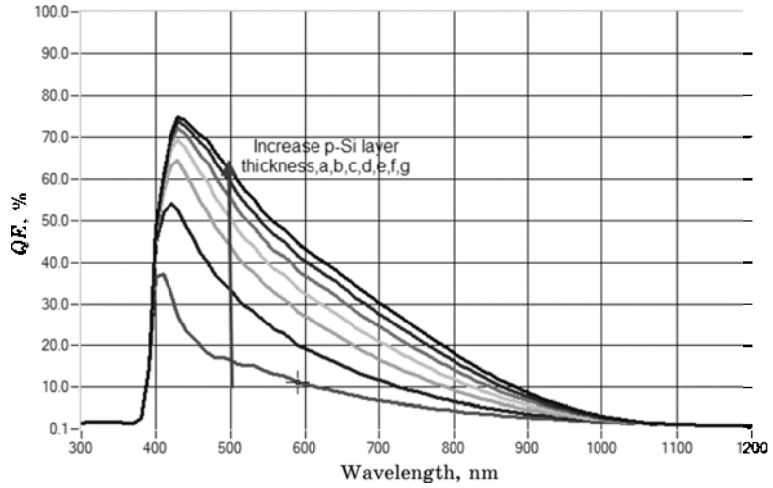

Fig. 5. Quantum efficiency of *n*-ZnO/*p*-Si solar cell at various Si absorber layer thickness: *a* = 0.1 um, *b* = 0.5 um, *c* = 1 um, *d* = 1.5 um, *e* = 2 um, *f* = 2.5 um, *g* = 3 um; *n*-layer = 3 um; Na = Nd = 10^{19}.

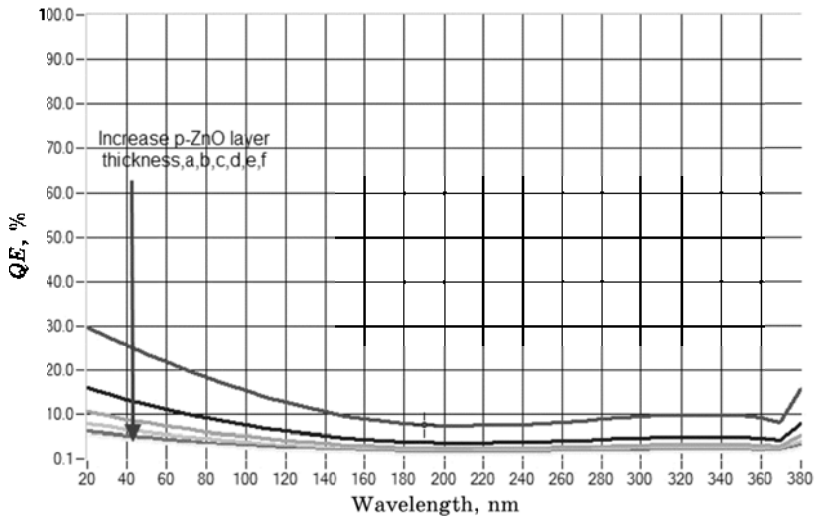

Fig. 6. Quantum efficiency of *n*-ZnO/*p*-Si solar cell at various ZnO absorber layer thicknesses: $a = 0.1$ um, $b = 0.3$ um, $c = 0.5$ um, $d = 0.75$ um, $e = 1$ um, $f = 2$ um; *p*-layer = 3 um; Na = Nd = 10^{18}.

larger number of photons to be absorbed and contribute into the EHP generation. In addition, the generation process will occur far from the high-recombination back-contact region and near the SCR, so that the quantum efficiency has been increased with the thickness of *p*-Si absorber layer in the range of $\lambda = 380–1200$ nm.

5.2. Effect of *n*-ZnO Thickness

The effect of the thickness variation of the *n*-ZnO layer on the light *J*–*V* curves of the *n*-ZnO/*p*-Si solar cell is shown in Fig. 4, where the thickness of *n*-ZnO layer has been varied from 0.5 to 3 um.

As shown in Fig. 4, both V_{oc} and J_{sc} values have been decreased, when the thickness of *n*-ZnO layer increased, and as the thickness of *n*-ZnO layer increased, more photons, which carry the energy ($h\nu \geq E_{g(ZnO)}$), are being absorbed by the layer. Therefore, it will lead to decrease in the number of photons, which could reach the absorber layer. Therefore, both V_{oc} and J_{sc} have been decreased.

The reduction in V_{oc} and J_{sc} will cause reduction in ($\eta\%$).The effect of the thickness of the ZnO layer on the O/P parameters of the cell is listed in Table 3.

The reduction in the number of photons in the absorber layer, which have energy greater than the energy band gap of the ZnO layer, will decrease the quantum efficiency in the region between $\lambda = 20–380$ nm, as shown in Fig. 6.

TABLE 3. J–V parameters of n-ZnO/p-Si solar cell at various ZnO absorber layer thickness.

No.	Thickness ZnO, um	V_{oc}, Volt	J_{sc}, mA/cm^2	FF, %	η, %
a	0.1	0.4639	13.058	77.04	4.6
b	0.3	0.4638	12.765	77.18	4.5
c	0.5	0.4638	12.675	77.22	4.5
d	0.75	0.463	12.623	77.21	4.5
e	1	0.463	12.59	77.2	4.5
f	2	0.4	12.5	80.35	4.5

5.3. Effect of Doping Density

The effect of the doping density of the p-Si absorber layer for both 0.5 um and 3 um absorber thicknesses is listed in Tables 4, 5.

TABLE 4. Effect of the doping density of the p-Si absorber layer (0.5 um), Nd = 10^{19}.

Doping density, Na	V_{oc}, Volt	J_{sc}, mA/cm^2	FF, %	η, %
1E+16	0.252	6.657	62.82	1.06
1E+17	0.346	6.461	72.05	1.61
1E+18	0.414	6.364	76.55	2.02
1E+19	0.477	6.328	78.43	2.37
1E+20	0.543	6.06	71.89	2.37

TABLE 5. Effect of the doping density of the p-Si absorber layer (3 um), Nd = 10^{19}.

Doping density, Na	V_{oc}, Volt	J_{sc}, mA/cm^2	FF, %	η, %
1E+16	0.33	12.893	72.16	3.06
1E+17	0.401	12.69	76.28	3.88
1E+18	0.464	12.609	78.98	4.62
1E+19	0.525	12.578	80.35	5.31
1E+20	0.587	12.451	79.66	5.83

The impact of the doping density of the Si layer on the light J–V curves is shown in Fig. 7 for absorber thickness of 0.5 um and in Fig. 8 for absorber thickness of 3 um. Increasing of the doping density of the Si decreases the space charge region width, so, the electric field in the depletion layer will increase .This will result in an increasing in V_{oc} for 3 um and 0.5 um absorber layer thickness.

When the electric field in the SCR increases, the diffusion length of

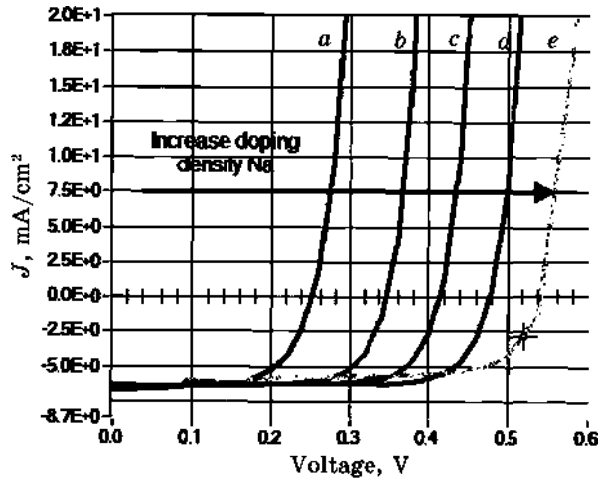

Fig. 7. Effect of the doping density of the *p*-Si absorber layer for both (0.5 um) absorber thickness.

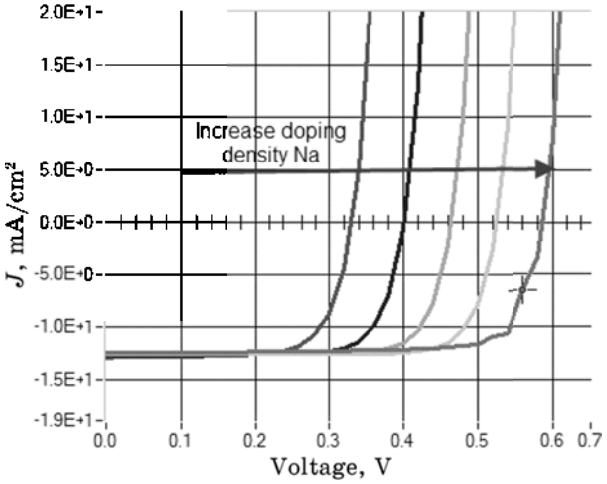

Fig. 8. Effect of the doping density of the *p*-Si absorber layer for both (3 um) absorber thicknesses.

the generated carriers also increases. Therefore, the photogenerated carriers will approach from the high-recombination back-contact region. This will lead to reduction in J_{sc}, as shown in Fig. 9, for the *p*-Si absorber layer of 0.5 um, *n*-ZnO layer thickness of 3 um, and this reduction will become more pronounced for very thin absorber, as shown in Fig. 10 for *p*-Si absorber layer of 3 um *n*-ZnO layer thickness of 3 um.

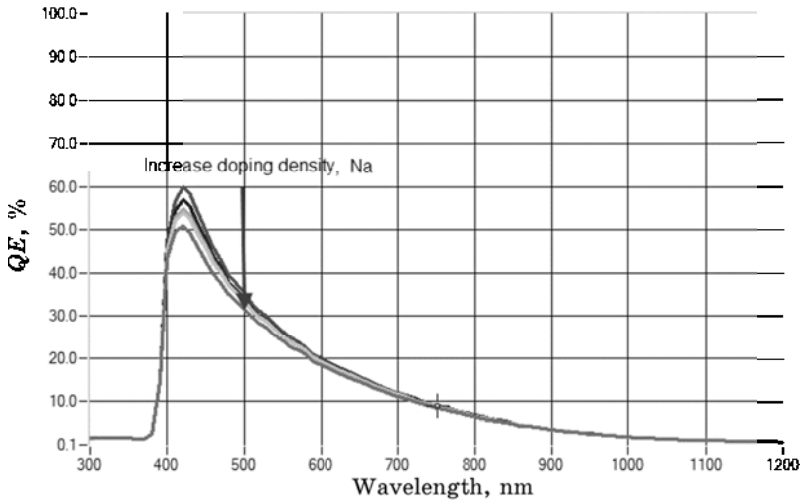

Fig. 9. Effect of the increased doping density on the *QE* of the *p*-Si absorber layer (0.5 um), *n*-ZnO layer thickness (3 um), Nd = 10^{19}, Na = 10^{16}–10^{20}.

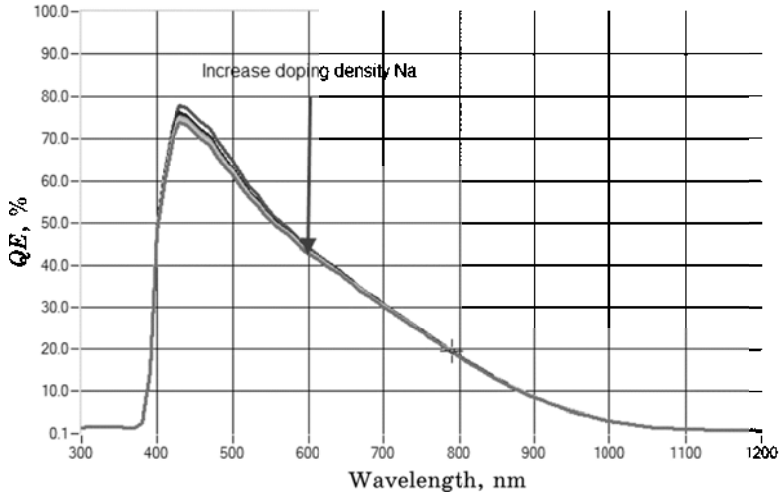

Fig. 10. Effect of the increased doping density on the *QE* of the *p*-Si absorber layer (3 um), *n*-ZnO layer thickness (3 um), Nd = 10^{19}, Na = 10^{16}–10^{20}.

For thin Si absorber layer of 0.5 um, the η% will increase with increasing in the doping density due to the reduction in J_{sc}, and for thickness of 3 um, the η% will increase with the doping density due to the increment in V_{oc}.

The generated EHP will reach the high-recombined back-contact region; for high electric field, due to the doping density, this will reduce

quantum efficiency of the device, when the doping is increased. The effect of the increased doping density on the *QE* is shown in Fig. 10.

6. PRACTICAL RESULTS

Let us compare our simulation results with the practical results obtained in [7], as shown in Tables 6 and 7.

TABLE 6. Output of practical illumination result for *n*-ZnO/*p*-Si solar cell [7].

Type	V_{oc}, Volt	J_{sc}, mA/cm^2	FF, %	η, %
n-ZnO/*p*-Si	0.35	19	50	4.33

TABLE. 7. Simulation result for *n*-ZnO/*p*-Si solar cell in light at room temperature and *n*-, *p*-layer thickness equal (1.3 um).

Type	V_{oc}, Volt	J_{sc}, mA/cm^2	FF, %	η, %
n-ZnO/*p*-Si	0.525	11.675	78.52	4.81

The light *J*–*V* curve obtained from the simulation study is shown in Fig. 11.

The difference between the simulation and the practical study was caused by interface state and surface recombination included in a real

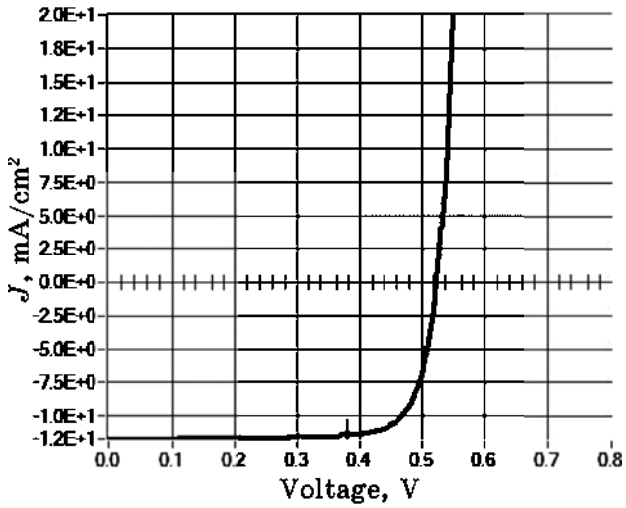

Fig. 11. *J*–*V* simulation curve of *n*-ZnO/*p*-Si heterojunction solar cell on light, at room temperature and *n*-, *p*-layer thickness equal (1, 3), respectively; Na = 10^{19}, Nd = 10^{16}.

device. The parameters resulting from the simulation study are listed in Table 7.

7. CONCLUSION

Intrinsic material properties, including band gap, working temperature, layers thickness, and doping percentage, are important factors influencing J–V characteristics of the n-ZnO/p-Si heterojunction solar cell. The comparison results for practice and simulation illustrate nearly same results. Then, we obtained the best results of 5.83% with $V_{oc} = 0.589$ V, $J_{sc} = 12.451$ mA at 300 K, Na = Nd = 10^{19}.

REFERENCES

1. R. H. Bube, *Photovoltaic Materials* (Imperial College Press: 1998).
2. M. Kemell, *M. Sci. Thesis* (University of Helsinki: 2003).
3. B. Joseph, P. K. Manoj, and V. K. Vajdyan, *Bull. Mater. Science*, **28**, No. 5: 487 (2005).
4. H. Kobayashi, H. Mori, and Y. Ishida, *Appl. Phys.*, **77**: 301 (1995).
5. M. Burgelman, P. Nollet, and S. Degrave, *Thin Solid Films* (Elsevier: 2000).
6. M. Burgelman, *SCAP User Manual* (ELIS University of Grn.: 2007).
7. H. H. Affify and S. H. Hefnawi, *Egypt. J. Solids*, **28**, No. 2: (2005).